Structure of Yeast Poly(A) Polymerase and its Complex with 3′-dATP

The structure of Polyadenylate [poly(A)] polymerase (PAP) and its complex with 3′-deoxyadenosine triphosphate (3′-dATP) was refined to 2.6 Å using selenomethionine multiwavelength anomalous diffraction (MAD). The crystal structure of the PAP from *Saccharomyces cerevisiae* looks like many other polymerases. A large 20 Å × 30 Å × 45 Å cleft is bounded by three globular domains; however, the thumb domain is missing.

Polyadenylate [poly(A)] polymerase (PAP) catalyzes the addition of a polyadenosine tail to almost all eukaryotic messenger RNAs (mRNAs). The crystal structure of the PAP from *Saccharomyces cerevisiae* (Pap1) has been solved to 2.6 Å, both alone and in complex with 3′-deoxyadenosine triphosphate (3′-dATP). Diffraction data for Pap1 in complex with 3′-dATP and Mn^{2+} were collected using the experiment facilities of beamline 19-ID of the Structural Biology Center (SBC) at Argonne's Advanced Photon Source (APS). Like other nucleic acid polymerases, Pap1 is composed of three domains that encircle the active site. The arrangement of these domains, however, is quite different from that seen in polymerases that use a template to select and position their incoming nucleotides. The first two domains are functionally analogous to polymerase palm and fingers domains. The third domain is attached to the fingers domain and is known to interact with the single-stranded RNA primer. In the nucleotide complex, two molecules of 3′-dATP are bound to Pap1. One occupies the position of the incoming base prior to its addition to the mRNA chain. The other is believed to occupy the position of the 3′ end of the mRNA primer.

Polyadenylation provides a universal handle by which transport and translation machinery can recognize and physically manipulate mRNAs. In eukaryotic organisms, addition of the poly(A) tail facilitates the transport of mRNA from the cell nucleus and helps regulate mRNA stability. Interactions between proteins bound to the poly(A) tail and the 5' end of mRNA in the cytoplasm are thought to cause circularization of the message and increase the efficiency of translation. Polyadenylation of mRNA is also observed in prokaryotes and appears to facilitate mRNA degradation.

Poly(A) tails are formed by a multiprotein complex, which recognizes a polyadenylation signal at the 3′ end of a nascent transcript and cleaves the precursor RNA. PAP then adds the poly(A) tail. PAPs are well conserved across phyla, with the first ~400 amino acids showing considerable sequence identity. The catalytic function of PAP resides in its NH_2-terminal domain, which shows sequence similarity to members of the nucleotidyl transferase (NT) family that includes DNA polymerase β (Polβ), CCA-adding enzymes, and several bacterial antibiotic-resistance enzymes. Pap1 retains polymerase activity when separated from the holoenzyme assembly and can processively add long stretches of adenosine nucleotides to an RNA primer *in vitro*. Although it employs the same catalytic mechanism as other nucleic acid polymerases, PAP is significantly different in that it does not use a template strand to select and position the incoming nucleotide.

The x-ray structure of both the apo and 3′-dATP-bound states of a Pap1 truncation mutant (Δ10PAP), which contains the NH_2-terminal 537 of

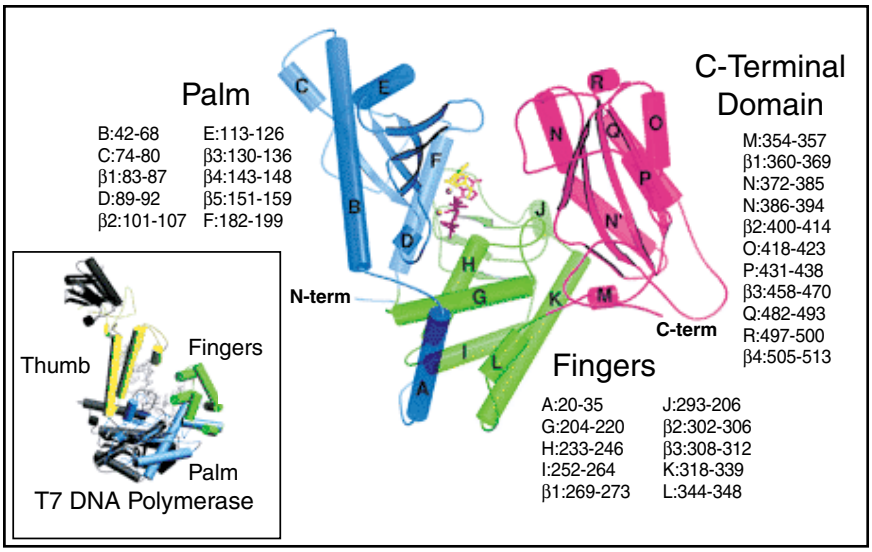

FIG. 1. Schematic view of Pap1. Residues 2 to 199 are shown in blue, 200 to 350 in green, and 251 to 530 in purple. The model is based on molecule B of the two independent copies of Pap1 in the asymmetric unit; residues 445 to 456 and 473 to 478, not modeled in molecule B, are based on the equivalent residues from molecule A. Two divalent cations (orange) are shown bound to the active site and to the phosphates of the incoming 3′-dATP (red). The mononucleotide primer is shown in yellow. A model of T7 DNA polymerase [1T7P] is shown (inset) for comparison.

the 568 amino acids in wild-type Pap1, was determined. This truncated enzyme exhibits wild-type activity *in vitro* and is capable of rescuing an otherwise lethal disruption of the yeast PAP1 gene. Crystals of Δ10PAP contain two copies of Pap1 in the asymmetric unit of the unit cell. The structure was solved to 3.2 Å by selenomethionine multiwavelength anomalous diffraction (MAD). The structure was later refined against higher resolution data sets with and without 3′-dATP and divalent cations soaked into the crystals; data from the latter complex were collected at SBC beamline 19-ID located at the APS. Table I summarizes crystallographic data collection and refinement statistics for the Δ10PAP/3′-dATP complex.

At first glance, Pap1 looks like many other polymerases. A large 20 Å × 30 Å × 45 Å cleft is bounded by three globular domains (Fig. 1). In other polymerases, this arrangement has been likened to a hand in which the substrates are held between the thumb and fingers and presented to an active site in the palm (Fig. 1, inset). Pap1 differs from these polymerases, however, in that the thumb domain is missing. The catalytic palm domain forms a wall of the cleft rather than sitting at its base. The base of the cleft interacts with the phosphate groups of the incoming nucleotide and is therefore functionally analogous to the fingers domains of other polymerases. The COOH-terminal domain forms the other wall of the cleft. Specificity determinants near

Table I. Data and refinement summary for the ΔPAP/3′–dATP complex.

		Pap1 with 3′-dATP and Mn^{2+}
Space group [cell dimensions]		$P2_12_12_1$ [73.8 Å, 109.1Å, 238.5Å]
Molecules per asymmetric unit		2 [537 amino acids per molecule]
Solvent content (%)		70
X-ray source		SBC beamline 19-ID (APS)
Resolution limit (Å)		2.6
Observed [unique] reflections		242,159 [58,367]
Completeness [last shell] (%)		97.8 [99.9]
R_{sym} [last shell] (%)		4.4 [39.7]
1/σ [last shell]		32.4 [2.8]
R_{work} [R_{free}] (%)		23.3 [27.9]
rms deviation from ideality:	Bond lengths (Å)	0.007
	Bond angles (°)	1.35
	Dihedral angles (°)	22.3
Water molecules modeled		83
Residues modeled:	Molecule A	3–427, 440–523
	Molecule B	2–444, 457–472, 479–530
Protein Data Bank accession number		1FA0

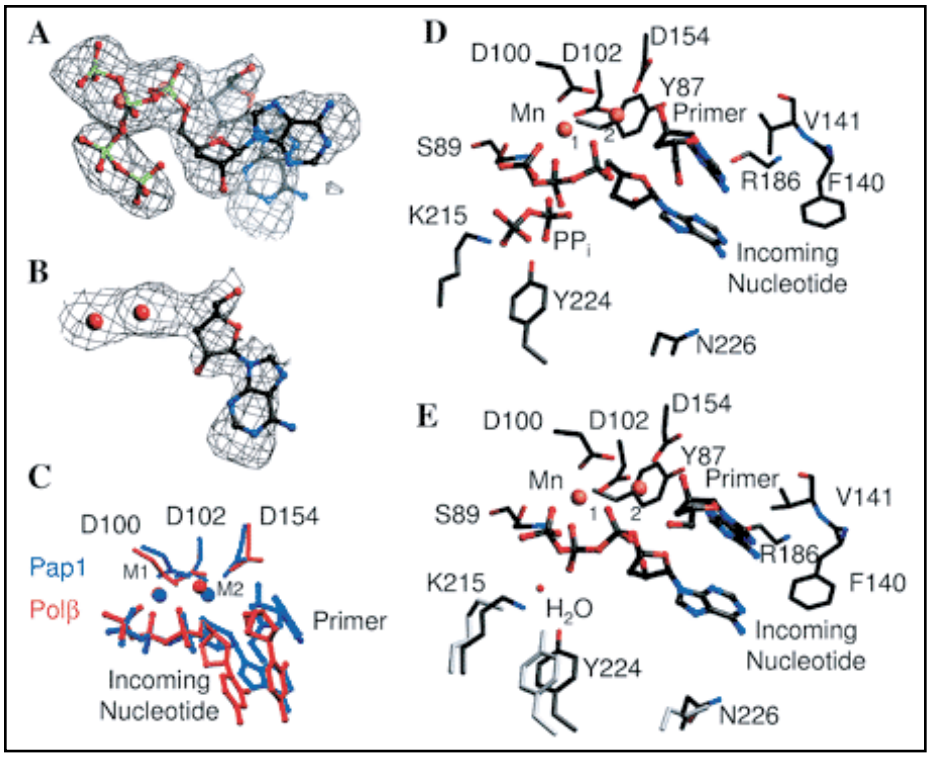

FIG. 2. Geometry of the active site. (a) $F_o - F_c$ simulated annealing omit map contoured at 2.5 σ showing electron density corresponding to the incoming 3′-dATP and PP_i in molecule A. Additional density corresponding to the mononucleotide primer is visible in the background. (b) View of the electron density for the mononucleotide primer in the same map. Two Mn^{2+} atoms are shown in red. Only the adenine and ribose of this nucleotide are modeled. The phosphates were not visible in the electron density and are assumed to be disordered. (c) Superposition of the active sites of Pap1 (blue) and Polβ (red) [1BPY] based on the side chains of the three catalytic aspartates. (d) Model of the active site from molecule A. (e) Model of the same region of molecule B. The positions of lysine-215, tyrosine-224, and asparagine-226 in molecule A are shown in light gray for reference.

the NH_2- and COOH-termini of Δ10PAP are known to interact with other components of the 3′ end processing machinery. These regions are on opposite sides of the structure, consistent with biochemical evidence that they function independently in regulating Pap1 activity.

The palm domain of Pap1 is structurally similar to the palms of other members of the NT family of proteins. Three conserved acidic residues (aspartate-100, -102, and -154) coordinate the two metal ions required for catalysis. These metal ions and the incoming nucleotide are clearly visible in difference maps calculated using the native data and data from crystals soaked in 3′-dATP and $MnCl_2$ (Fig. 2a). The positions of the metal ions and phosphates correspond well with those observed in the active complex of Polβ (Fig. 2c). Although the metals and phosphates exhibit very strong electron density, that of the ribose and base is weaker, suggesting that these parts of the substrate may be flexible.

Electron density consistent with the presence of the sugar and base of a second 3′-dATP molecule is also observed (Figs. 2a and 2b). Like that of the incoming nucleotide, the position of this density is very similar in both crystallographically independent copies of the complex. The second nucleotide occupies the position where the 3′ end of the primer would be expected based on the Polβ structure. The bases of the two nucleotides do not appear to stack but are close enough to allow hydrogen bonding between N6 of the primer and N3 of the incoming nucleotide. This interaction, however, does not satisfactorily explain the selectivity of Pap1 for ATP as the incoming nucleotide. In other polymerases, formation of a correct base pair between the incoming nucleotide and the template is only detected in the "closed" conformation of the palm and fingers domains. It may be that Pap1 adopts a similar closed conformation during the catalytic cycle. Slight rotation of the fingers domain relative to the palm could place the conserved residue asparagine-226 within hydrogen-bonding distance of the adenosine-specific N6 atom of the incoming nucleotide.

In contrast to the incoming nucleotide triphosphate, the mononucleotide primer shows extensive interactions with Pap1 (Figs. 2d and 2e). The base of the primer 3′-dATP molecule stacks against the functionally important residue valine-141. When the

palm domains of Pap1 and Polβ are superimposed, Pap1 phenylalanine-140, which sits at the apex of the β-hairpin-containing valine-141, occupies the same position as the +1 nucleotide of the Polβ template DNA. This β-hairpin may thus serve to compensate for the absence of a template in binding and positioning the primer. In addition, a hydrogen bond between the N6 amino group of the primer base and the main chain carbonyl of arginine-186 could select for adenine over guanine.

The two crystallographically independent molecules (molecule A and molecule B) differ by ~5° in the orientation of the palm relative to the fingers. Interactions between the fingers domain and the incoming nucleotide are strongly affected by this rotation. In molecule B, tyrosine-224 and lysine-215 are quite close to the incoming 3′-dATP, with the β-phosphate and lysine-215 coordinating a water molecule (Fig. 2e). Molecule A, however, is in a more open conformation, and tyrosine-224 and lysine-215 instead appear to interact with pyrophosphate, the by-product of the polymerase reaction (Figs. 2a and 2d). Lysine-215 may therefore function to neutralize the pyrophosphate anion after catalysis. It has been proposed that similarly positioned lysines assume an analogous role in *E. coli* DNA polymerase I and T7 DNA polymerase.

The COOH-terminal domain of Pap1 binds the RNA primer/product. Residues 525 to 537 define a COOH-terminal RNA binding site (C-RBS), which is required for Pap1 processivity and for ultraviolet cross-linking to the upstream region of the RNA primer. The C-RBS of Pap1 appears to be flexible, and the electron density beyond residues 523 and 530 in molecules A and B, respectively, cannot be modeled. Those residues of the C-RBS that have been modeled extend away from the cleft, perhaps explaining why cross-linking to the Pap1 C-RBS is not observed when RNA is labeled only at its 3′ end.

Adapted with permission from "*Structure of Yeast Poly(A) Polymerase Alone and in Complex with 3′-dATP*," Science, **289**, 1346–1349 (2000).

J. Bard,[1] A. M. Zhelkovsky,[2] S. Helmling,[2] T. N. Earnest,[3] C. L. Moore,[2] A. Bohm[1,4]

[1] *Boston Biomedical Research Institute, Watertown, MA, U.S.A.*
[2] *Tufts University School of Medicine, Department of Molecular Microbiology, Boston, MA, U.S.A.*
[3] *Macromolecular Crystallography Facility at the Advanced Light Source, Physical Biosciences Division, Lawrence Berkeley National Laboratory, Berkeley, CA, U.S.A.*
[4] *Tufts University School of Medicine, Department of Biochemistry, Boston, MA, U.S.A.*